THE CANADIAN MINERALOGIST
Journal of the Mineralogical Association of Canada

Volume 20 May 1982 Part 2

Canadian Mineralogist
Vol. 20, pp. 129-140 (1982)

DIAGENESIS OF THE NISKU FORMATION AND THE ORIGIN OF LATE-STAGE CEMENTS

CYNTHIA NAHNYBIDA, IAN HUTCHEON AND JILL KIRKER
Department of Geology and Geophysics, University of Calgary, Calgary, Alberta T2N 1N4

ABSTRACT

Late-stage calcite, dolomite and anhydrite cements, which occur in Upper Devonian dolostones of the Nisku Formation, west-central Alberta, have been examined using thin-section petrography, fluid-inclusion microthermometry, stable-isotope data and electron-probe microanalysis. The entire diagenetic sequence is interpreted to be: selective dissolution of fossils, dolomitization, extensive stylolitization, precipitation of calcite cements before, during and after stylolitization, and late-stage anhydrite emplacement. Fluid-inclusion data indicate that the late calcite cements were deposited at temperatures of between 140 and 155°C from solutions approximately 2.4–3.7 *m* NaCl (equivalent). At the present depth of burial of 2.5 km and H_2O activities estimated from NaCl-equivalent contents of the aqueous phase in fluid inclusions, the minimum temperature of dehydration of gypsum to anhydrite would range from 75°C (fluid pressure) to 135°C (lithostatic pressure). The temperature range determined in this study, though moderately high, is not inconsistent with published bore-hole temperatures and vitrinite-reflectance data. Gypsum was not observed; these temperatures would represent a minimum range at the 2.5 km burial depth. Isotopic data for sulfur and oxygen in both "early" and "late" anhydrites show a distinct separation and may indicate that sulfate, introduced into solution by dissolution of "early" anhydrite, was being reduced during the precipitation of "late" anhydrite.

Keywords: diagenetic conditions, carbonates, anhydrite, fluid inclusions, thermodynamics, stable isotopes, Nisku Formation, Alberta.

SOMMAIRE

On a étudié les ciments tardifs de calcite, dolomite et anhydrite des dolomies de la formation Nisku (Dévonien supérieur, partie centre-ouest de l'Alberta) par pétrographie en lames minces, microthermométrie au moyen d'inclusions fluides, géochimie des isotopes stables et microanalyses à la microsonde. La séquence complète de diagenèse serait la suivante: dissolution préférentielle des fossiles, dolomitisation, stylolitisation très étendue, déposition d'un ciment calcitique avant, pendant et après la stylolitisation, et mise-en-place tardive de l'anhydrite. Les inclusions fluides montrent que la cimentation tardive par la calcite impliquait une solution contenant entre 2.4 et 3.7 *m* de NaCl (concentration équivalente) à une température comprise entre 140 et 155°C. Aux profondeurs d'enfouissement actuelles de 2.5 km et à des valeurs d'activité de H_2O qui concordent avec la composition de la phase aqueuse dans les inclusions fluides (en termes d'équivalences de NaCl), la température minimum de déshydratation du gypse en anhydrite pourrait varier de 75°C (pression fluide) à 135°C (pression lithostatique). Quoiqu'elles sont relativement élevées, ces températures ne sont pas incompatibles avec celles que l'on enregistre dans les sondages ou que l'on calcule à partir de la réflectivité de la vitrinite. Aucun indice de gypse n'a pu être décelé. Ces températures représenteraient une marge minimum pour un enfouissement de 2.5 km. Les données isotopiques sur soufre et oxygène distinguent bien les générations précoce et tardive d'anhydrite; on en conclut que le sulfate libéré en phase aqueuse par dissolution de l'anhydrite précoce aurait été réduit pendant la formation d'anhydrite tardive.

(Traduit par la Rédaction)

Mots-clés: conditions diagénétiques, carbonates, anhydrite, inclusions fluides, thermodynamique, isotopes stables, formation Nisku, Alberta.

INTRODUCTION

Textural relationships are used to decipher the relative age of pore-filling cements in car-

bonate rocks. Exactly when any cement in a carbonate rock formed can rarely be determined. One method of recognizing how late a "late" cement in a rock formed is to try to determine the physical and chemical conditions that prevailed during precipitation of the cement. These conditions are related to the environment of diagenesis and give some indication of the stage of burial, during which cement precipitation occurred.

In this study, samples of core from the Nisku Formation in west-central Alberta (LSD 10-15-52 8W5, CDC Oil and Gas) were collected over a 98-m-interval (2270–2368 m). Thin-section petrography, X-ray diffraction, electron-probe microanalysis, stable-isotope geochemistry and fluid-inclusion measurements were all employed to aid in understanding the conditions of diagenesis. The studied well, which was the subject of an intensive geological, geophysical and geochemical investigation by Chevron Exploration (1979), is located in the West Pembina area in an off-reef position (Fig. 1). Samples studied are from the Zeta Lake and Lobstick (platform) members of the Nisku Formation (Fig. 2).

General Lithology and Mineralogy

The bottom 10 m of the core (2358–2368 m) are composed of nodular, argillaceous limestone and fossiliferous floatstone containing coral, crinoids, stromatoporoids and brachiopods. Only minor dolomitization has occurred, and pyrite is the most abundant late-diagenetic mineral. The precipitation of pyrite, primarily in open spaces, resulted in an overall reduction of porosity. This portion of the core is interpreted as reef platform (Fig. 3) and is probably part of the Lobstick Member. Little mention will be made of the platform sediments in the remainder of this paper.

The bulk of the core samples are from a Zeta Lake Member pinnacle reef, which is basinward of the main reef platform (Fig. 1). The lithologies consist of floatstone, wackestone and mudstone. The framework fossils are tabular stromatoporoids and branching corals, with brachiopod and crinoid fragments being common constituents of the matrix.

Generally, the reef section is very porous, although the distribution of porosity varies considerably with rock type and extent of late-diagenetic cementation. Intercrystalline porosity, due to dolomitization of the matrix, contributes significantly to the overall porosity of the reef. The most conspicuous porosity is moldic or vugular, resulting from the selective dissolution of fossils, but much of this porosity is occluded by late-diagenetic calcite and anhydrite cements. These cements are the material examined in this study.

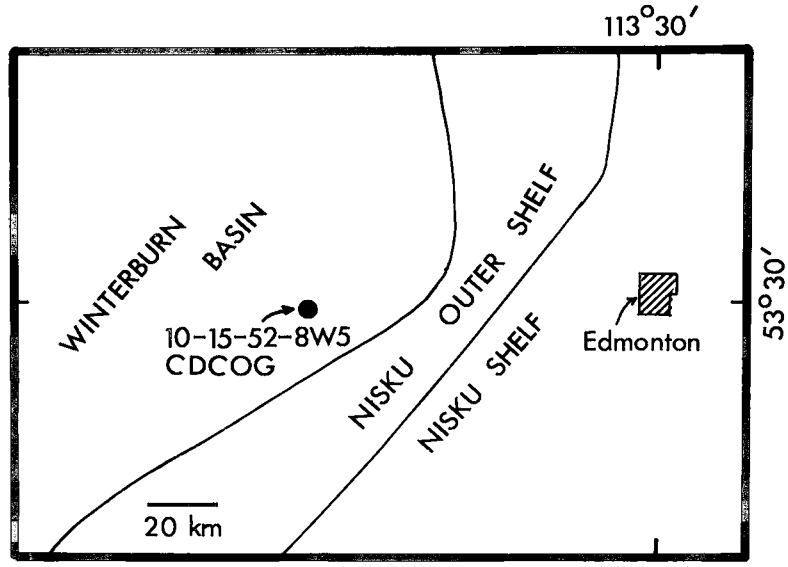

Fig. 1. Location of the CDCOG 10-15-52-8W5 well with respect to the Nisku shelf and the Winterburn basin.

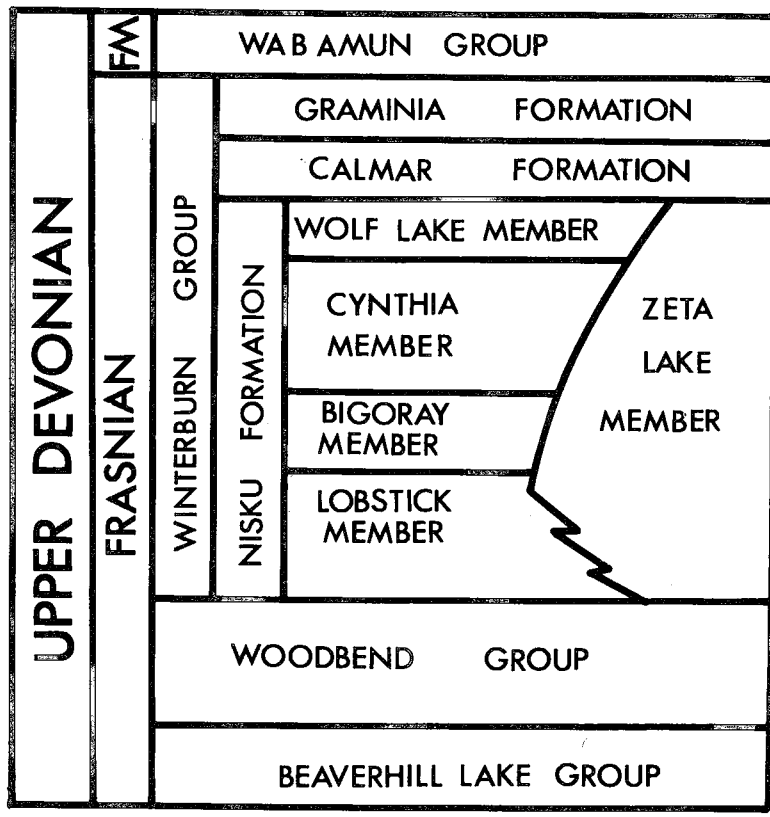

FIG. 2. Stratigraphic nomenclature of the Upper Devonian in central Alberta, showing the relationship of the Nisku Formation and Zeta Lake Member to other units.

PETROGRAPHY

Dolomite

Throughout the reef portion (Zeta Lake) of the core, the matrix is composed of brown, cloudy, subhedral to euhedral dolomite crystals, ranging in size from 0.005 to 0.1 mm. Patches of finer and coarser dolomite may reflect differences in the original grain-size of the sediment or indicate the amount of open space available for crystal growth. The latter case is apparent along the edges of vugs, where large, rhombohedra of dolomite up to 2.5 mm across have developed (Fig. 4). The interiors of these crystals are identical to the matrix dolomite in texture, and both are assumed to have formed during the same dolomitizing event. White syntactic overgrowths on the dolomite that lines the vugs may have been precipitated from the same solutions that dolomitized the matrix, or from later solutions. The clear, outermost zone on most dolomite overgrowths is iron-rich, as indicated by a potassium ferricyanide stain. On some dolomite crystals a second, discrete iron-rich zone was observed. Evamy (1969) suggested that the transition from low to high iron contents in carbonate cements reflects a change from oxidizing (vadose) conditions to reducing (phreatic) conditions. An alternative explanation for changes in iron content is the fluctuation of pore-water chemistry in response to changing diagenetic conditions during burial (Oldershaw & Scoffin 1967, Wong & Oldershaw 1981). None of the petrographic evidence favors one explanation over the other.

Some of the vugs in the central portion of the core show geopetal structures (Fig. 5), implying that selective dissolution of fossils took place early in the diagenetic history. The silt appears to have been deposited in the voids prior to at least one dolomitizing event, as coarse, zoned, Fe-rich rhombohedra of dolomite have crystallized on top of the silt (Fig. 5).

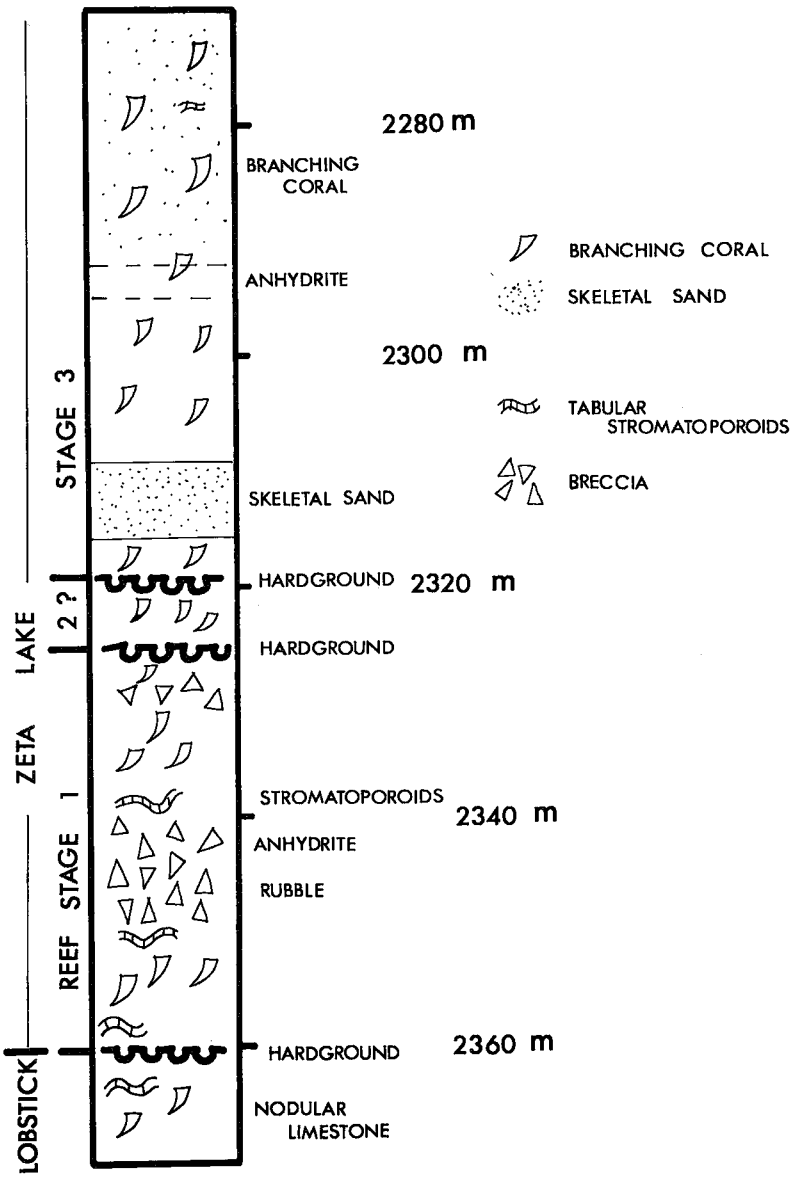

FIG. 3. Generalized description of the core examined in this study. Most samples are from the Zeta Lake Member.

Calcite

Coarse, white subhedral to anhedral calcite cement partly or completely fills many vugs and is later than the coarse dolomite (Fig. 5). The calcite crystals range from 0.5 to 5.0 mm and are clear, except for 5–20 μm fluid inclusions. The textural relationships between the dolomite and calcite cements are everywhere consistent with the coarse calcite being the later cement.

Calcite cements, most common in portions of the core that contain numerous stylolites, display various textural relationships: (1) calcite cement may be cross-cut by stylolites; (2) stylolites may be cross-cut by calcite cements, and, most commonly, (3) calcite cement is distributed either above or below a stylolite (Figs. 6, 7). Some calcite also exhibits undulose extinction and kinked twin lamellae, implying that the calcite was deposited during the period when stresses associated with stylolitization were

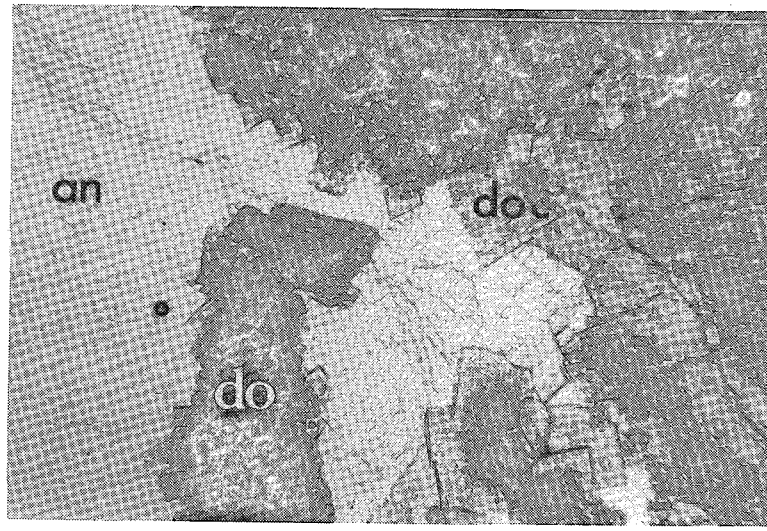

FIG. 4. Euhedral dolomite cements (doc) have developed on the rims of vugs in the dolomitic matrix (do). The open spaces are filled with anhydrite (an) or calcite (Fig. 5). Note the cloudy interiors of the euhedral dolomite. The bar represents 1 mm.

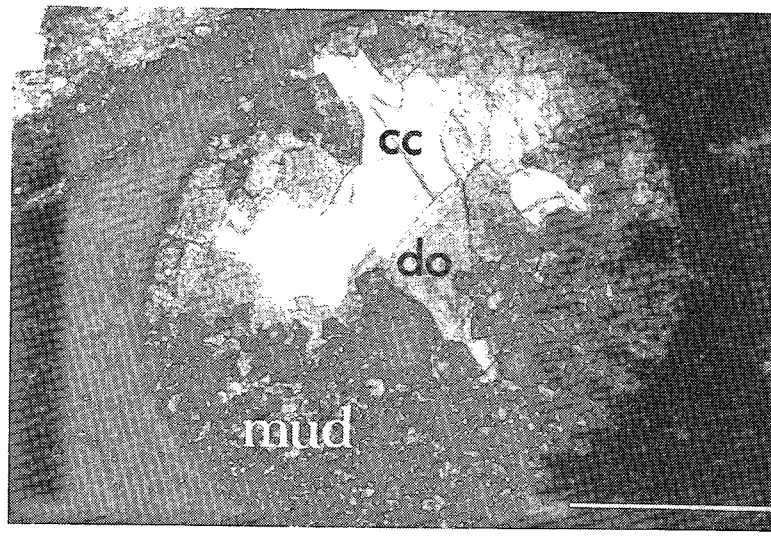

FIG. 5. The dolomitizing event responsible for the pore-lining euhedral dolomite (do) postdates the emplacement of muds within the vugs of the original rock. Note that euhedral dolomite has crystallized on top of mud (mud) that shows a geopetal structure. In this section the latest cement is calcite (cc). The bar represents 1 mm.

affecting the rock. It is probable that the material for the calcite cements was first dissolved along the stylolite and precipitated in vugs adjacent to the stylolite. The argillaceous material in the stylolites, rather than being a passive accumulation of insoluble material, may provide a chemical environment which, during progressive diagenesis, promotes the dissolution of carbonates.

Anhydrite

Anhydrite was observed in two different tex-

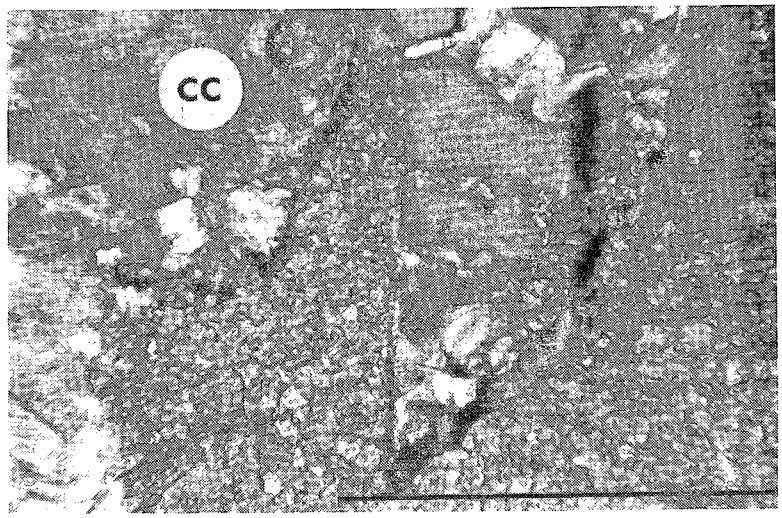

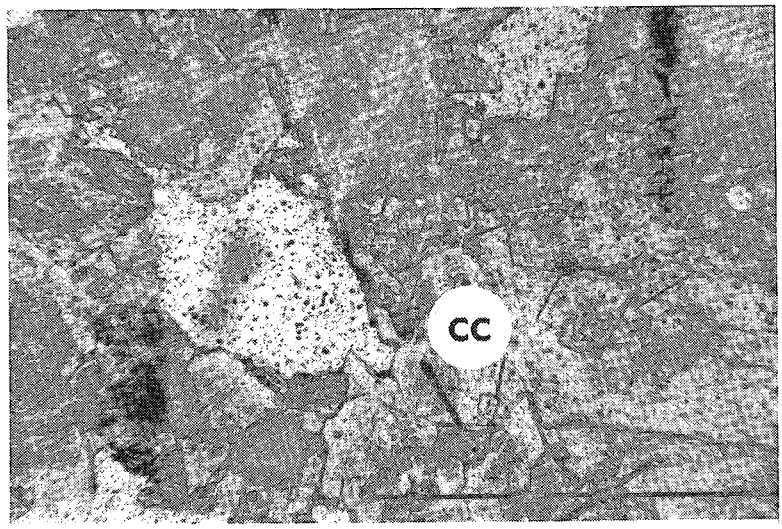

FIGS. 6, 7. Late calcite cements (cc) occur either above (Fig. 6) or below (Fig. 7) stylolites. The bar represents 1 mm.

tural forms within the Zeta Lake Member. One form occurs as white, fine-grained mats of anhydrite crystals in nodular patches up to 0.3 m in thickness. In thin section, acicular 0.5 mm (or less) crystals can be observed. Some early moldic porosity is filled with this type of anhydrite. The euhedral dolomite rhombs, lining the moldic pore cavities, appear to deform the alignment of anhydrite crystallites (Fig. 8). Either the anhydrite was forced into the cavity as a solid or dolomite growth postdates this anhydrite.

The second mode of occurrence of anhydrite is in the form of bladed crystals up to 10 mm in length (Fig. 9) that fill dolomite-lined vugs and, by textural criteria, are later than the nodular anhydrite. Calcite and anhydrite were rarely observed in contact with each other, but in one thin section, bladed anhydrite occludes a vug partially filled with calcite, implying that bladed anhydrite is contemporaneous with, or postdates, the coarse calcite cement. Anhydrite was observed adjacent to or cross-cutting stylolites, implying that it is slightly later than cal-

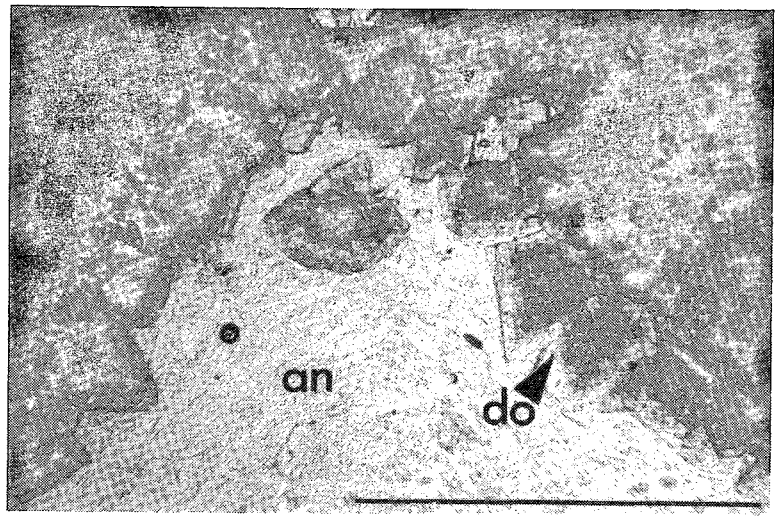

FIG. 8. Some anhydrite (an) appears to be displaced by the growth of euhedral dolomite (do). The texture is compatible with anhydrite having been forced into the pore space. The bar represents 1 mm.

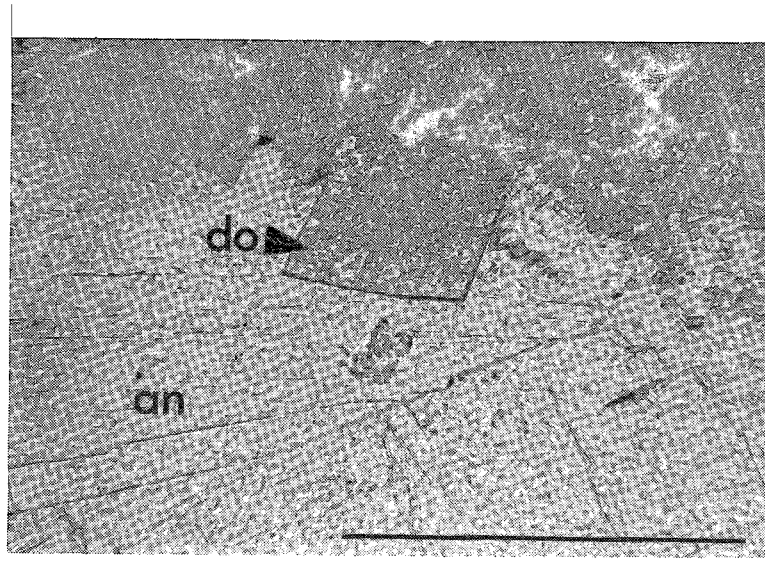

FIG. 9. The late anhydrite (an) is very coarse grained and is not displaced by the pore-lining dolomite (do). The bar represents 1 mm.

cite (which cuts and is cut by stylolites). Definite timing relationships are difficult to establish.

Pyrite

Pyrite is present in most samples as fine-grained irregular masses of subhedral to euhedral crystals. It is associated with early, massive anhydrite and fossil fragments, occurs along stylolites and, in places, cross-cuts dolomite, calcite, and anhydrite cements. It appears that pyrite has formed at many stages during diagenesis from the earliest to the latest events.

Hydrocarbons

Hydrocarbon staining was observed in two

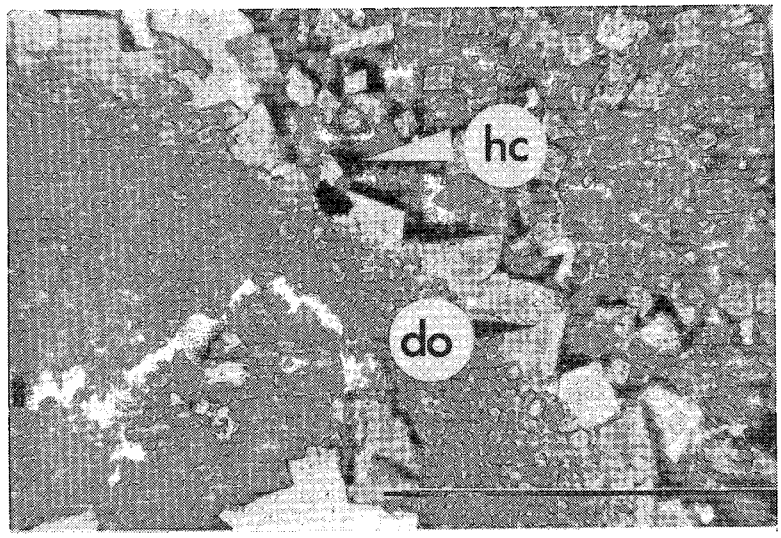

FIG. 10. Hydrocarbons (hc) fill the pore space in some parts of the section and appear to postdate the pore-lining euhedral dolomite (do). The presence of hydrocarbons in these pore spaces may have prevented further growth of cement material. The bar represents 1 mm.

thin sections (Fig. 10) and occurs in skeletal sands with good porosity. Entrapment of hydrocarbons in the pores is effected by rhombic dolomite, implying that migration postdates or is contemporaneous with this event. Where hydrocarbons are present, no stylolites were observed, leaving at least two possible interpretations: (1) hydrocarbon emplacement preceded stylolite formation and prevented infiltration of cementing fluids, thus preventing stylolite growth, or (2) stylolite formation and concurrent cementation closed off porosity, preventing hydrocarbon emplacement in parts of the rock more susceptible to stylolite growth. Either case is possible.

FLUID-INCLUSION MEASUREMENTS

As a mineral crystallizes, droplets of the fluid medium may be trapped, forming a primary fluid inclusion. A two-phase (liquid + vapor) fluid inclusion is presumed to indicate that fluid was trapped as a single phase at higher temperatures and, on cooling, the vapor phase exsolved from the liquid. On heating a two-phase fluid inclusion, the homogenization temperature can be observed and is assumed to represent the minimum temperature of the fluid during crystal growth. By calculation of the freezing-point depression, the temperature of final melting of a frozen fluid-inclusion can be related to the salinity (in NaCl equivalents) of the trapped solution. Homogenization and final melting temperatures were measured in this study using a Chaix–Meca heating–freezing microscope stage. Large (0.01 mm) isolated (*i.e.*, not on fractures) fluid inclusions in the late, clear calcite cement were assumed to be primary and used for such measurements. Examination under ultraviolet light indicated the inclusions are aqueous, rather than hydrocarbon-filled.

Temperatures of final melting were measured in triplicate on twenty-one primary inclusions in six samples that cover a range of depths (Table 1). Although the melting temperatures vary, there is no obvious trend with depth. Using an expression from Potter & Clynne (1978), the molalities of the aqueous phase, as NaCl equivalents, can be calculated. Molalities

TABLE 1. FINAL MELTING TEMPERATURES*

DEPTH (m)	N	FINAL Tm (°C)	m_s
2317.4	6	$-10.0^{\circ} \pm 2.0$	2.8 ± 0.6
2328.7	3	$-8.4^{\circ} \pm 1.3$	2.4 ± 0.4
2339.0	4	$-13.9^{\circ} \pm 2.0$	3.7 ± 0.6
2344.8	3	$-9.5^{\circ} \pm 2.7$	2.7 ± 0.8
2349.0	3	$-12.5^{\circ} \pm 0.4$	3.4 ± 0.1
2356.0	2	$-10.6^{\circ} \pm 1.6$	2.9 ± 0.5

* These temperatures are from two-phase fluid inclusions in calcite. The following abbreviations have been used: N = number of fluid inclusions measured; Tm = melting temperature; m_s = molality (equivalent NaCl).

ranging from 2.4 to 3.7 indicate the solutions responsible for calcite cementation were two to three times the concentration of seawater.

Homogenization temperatures were measured in triplicate on seventy-seven fluid inclusions in sixteen samples. As was found with the temperatures of final melting, there is no correlation with depth. Temperatures for each sample fall over a broad range, possibly indicating that calcite cements were deposited over a broad range of conditions. Because discrete growth-zones could not be detected in the calcite cement, it was not possible to determine whether homogenization or melting temperatures at any single stage of calcite precipitation were the same.

A histogram (Fig. 11) of homogenization temperatures exhibits a median value between 140 and 155°C; the mean of all homogenization temperatures is 144 ± 24°C. Assuming a geothermal gradient of 35°C/km (estimated from Derro *et al.* 1977), a burial depth of 3.6 km is suggested. Present depth is 2.3 km, and removal of 1.3 km of section is unlikely, given the

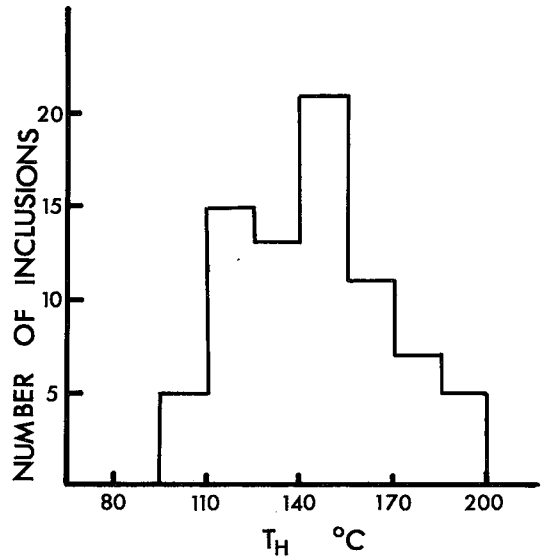

FIG. 11. Histogram of homogenization temperatures of primary fluid-inclusions in late-stage calcite cements.

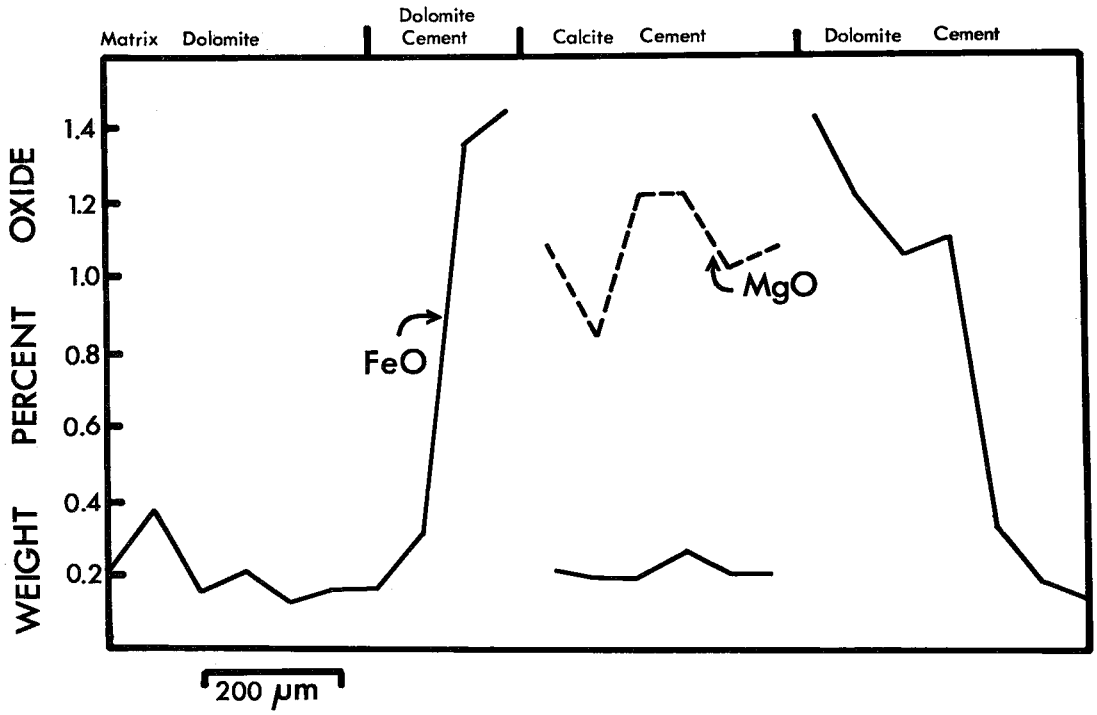

FIG. 12. The clear dolomite overgrowths have distinctly different iron contents than the matrix dolomite. The parts of the diagram labelled "dolomite cement" represent dolomite grains on each side of a single pore.

known stratigraphy. It is most likely that homogenization measurements are slightly high, but there may also have been some removal of stratigraphic section.

Chevron Exploration (1979) reports present-day reservoir temperatures of 75 to 120°C. Temperature measurements in boreholes are usually slightly lower than formation temperatures; thus paleotemperatures of 140°C do not seem excessive. Chevron also reports vitrinite-reflectance values of 0.5 to 1.1 (R_o^{max}%). According to Bostick (1979), this represents a potential temperature range between 100°C and 180°C. Fluid-inclusion temperatures of 144°C are therefore compatible with present temperatures and vitrinite-reflectance measurements.

Electron-Probe Microanalysis

The limited chemical data collected in this study are designed to aid in the qualification of timing relationships determined from petrography, rather than to describe in detail the chemistry of the cements. In this regard, the iron content of all carbonate minerals was found to be significant. Two traverses, with analyses at 60 μm intervals, were performed on each sample using an ARL–EMX microprobe. Compositional variation in one sample (depth 2320.5 m) is shown in Figure 12. Iron content averages 0.23 ± 0.12 wt. % FeO in the matrix dolomite and the cloudy cores of rhombic dolomite in pore-lining cements. The clear parts of the rhombic dolomite cements contain an average of 1.15 ± 0.13 wt. % FeO, with the transition between the two zones being very abrupt (Fig. 12). Discriminant-function analysis of matrix dolomite and core compositions of rhombic dolomite shows they are chemically indistinguishable, indicating that matrix dolomitization and the initial stages of dolomite cementation were simultaneous. The rapid change in composition of the clear dolomite overgrowths signifies a change in pore-water chemistry during dolomite growth.

The composition of the calcite cement is most similar to the matrix dolomite in FeO (0.15 ± 0.05 wt. %). Compositional fluctuations, which possibly reflect pore-water chemistry, are observed. Since the material for the calcite cement is believed to be derived from stylolitization (in part), these minor fluctuations may reflect input of the argillaceous material in the stylolites to the pore water.

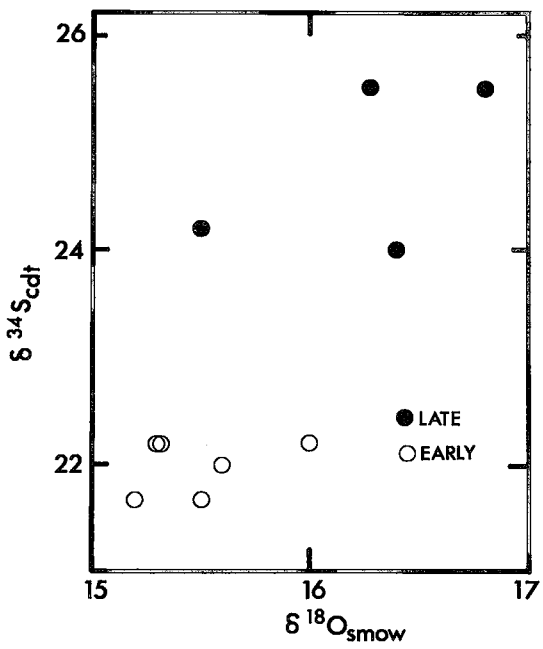

FIG. 13. The isotopic composition (oxygen relative to SMOW, sulfur relative to CDT) of "early" and "late" anhydrite. The "late" anhydrite has distinctly different sulfur isotopic values than the "early" sedimentary anhydrite.

Isotopic Composition of Anhydrite

Anhydrite occurs as early stratiform masses and later, as pore-space filling crystals. Samples of both types of material were separated for isotopic analyses performed by Asif Shakur. The normal δ notation is used to report isotopic values for sulfur (relative to Cañon Diablo troilite, CDT) and oxygen (relative to SMOW). In Figure 13 it is clear that the "early" anhydrite forms a distinct population from the late coarsely crystalline anhydrite. The average value for $\delta^{34}S$ in the early anhydrites is 22‰, approximately 2‰ lower than the average $\delta^{34}S$ reported by Claypool *et al.* (1980) for the Frasnian, but within the range of $\delta^{34}S$ of Frasnian-age sulfates. The "late" anhydrite averages 24.8‰ $\delta^{34}S$, very close to the average value of 24‰ reported by Claypool *et al.* (1980) and Sasaki & Krouse (1969). Petrographic evidence demonstrates two texturally distinct forms of anhydrite in these rocks. The stable isotopes, particularly $\delta^{34}S$, show some separation. It is, therefore, possible that careful petrographic observation of calcium sulfates will help to restrict the observed spread of $\delta^{34}S$ values of sulfates with time, by eliminating those data that are not obtained from primary sulfates.

Because pyrite appears with textural relationships indicating a very wide range of conditions

of formation, $\delta^{34}S$ data for pyrite would be unlikely to assist in the interpretation of the observed stable-isotope data for anhydrite. In addition, the $\delta^{34}S$ fractionation factor between anhydrite and water is a function of salinity and temperature. Interpretation of the observed $\delta^{34}S$ and $\delta^{18}O$ enrichment would require considerably more study. For our purposes, it is sufficient to recognize that the "early" and "late" generations of anhydrite are texturally and isotopically distinct and presumably reflect different modes (and times) of formation.

The Stability of Anhydrite

The late crystalline, pore-filling anhydrite probably formed late in the burial history and, according to fluid-inclusion-derived temperatures of final melting, precipitated from solutions three to four times the concentration of seawater. The dehydration temperature of gypsum to anhydrite, as a function of pressure and the activity of water, $a(H_2O)$, should provide a *minimum* estimate of diagenetic temperatures, since no gypsum is observed in the core. The equilibrium for the reaction

$$\underset{\text{gypsum}}{CaSO_4 \cdot 2H_2O} \rightleftarrows \underset{\text{anhydrite}}{CaSO_4} + 2H_2O \quad \ldots\ldots\ldots\ldots (1)$$

was calculated from data in Robie *et al.* (1978) and Keenan *et al.* (1969). The equilibrium constant for (1) is $K_1 = [a(H_2O)]^2$, assuming that anhydrite and gypsum are present as pure components. The calculated phase-relationships (Fig. 14) show the dehydration temperature of gypsum to be a function of water pressure and the activity of the component H_2O in the aqueous phase. Using equivalent NaCl concentrations estimated from fluid inclusions, the approximate activity of H_2O in the aqueous phase would be 0.9 (Robinson & Stokes 1959). Note that a standard state in which the activity of H_2O in the aqueous phase is unity at any pressure and temperature has been employed in these calculations. It is assumed that the decrease in $a(H_2O)$ with increasing salinity is not a function of temperature or pressure. If we assume that the late, pore-filling anhydrite formed at, or near, the maximum depth of burial of 2.5 km, the phase relations can be used to obtain a minimum temperature for anhydrite crystallization. At hydrostatic pressure, the minimum temperature of gypsum dehydration is 75°C. If the fluid attains lithostatic pressure, the minimum temperature of gypsum dehydration would be 120°C. The fluid pressure in the rock is probably higher than hydrostatic pressure; the minimum range of 75 to 120°C for anhydrite formation is in good agreement with fluid-inclusion data from the contemporaneous(?) calcite cements.

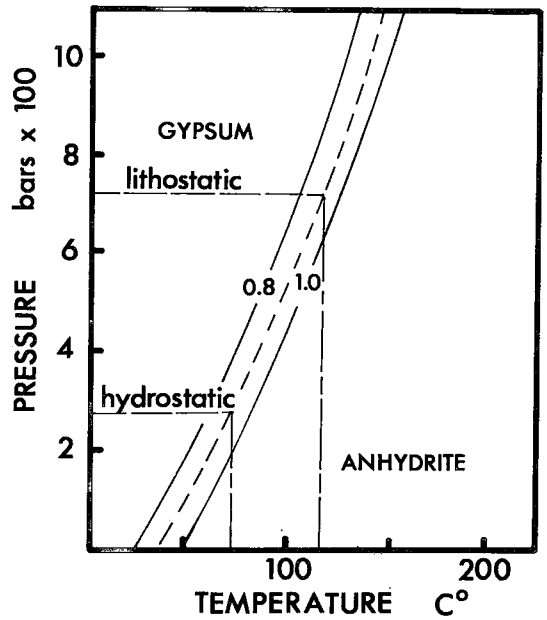

FIG. 14. The dehydration temperature of gypsum is a function of pressure and the activity of H_2O in the aqueous phase. The numbered contours show the position of the equilibrium between anhydrite and gypsum for $a(H_2O) = 1.0$ and 0.8. The dashed lines refer to the lithostatic and hydrostatic pressures at the present burial depth of 2.5 km.

Conclusions

The sequence of diagenetic events within the part of the Zeta Lake Member examined in this study is: selective dissolution of fossils, dolomitization, extensive stylolitization, precipitation of blocky calcite cements both preceding and postdating stylolites, and crystallization of late, pore-filling anhydrite.

The change in chemical composition of the euhedral, pore-lining, dolomite cements indicates that the outer Fe-rich parts formed at a distinct time, probably later than the dolomitization of the matrix. The cloudy cores of the euhedral dolomite crystals probably formed at the same time as the matrix dolomite.

The fluid-inclusion homogenization and final-melting temperatures indicate that the late calcite cements formed from solutions approximately three times the concentration of seawater and at temperatures of about 140°C.

Whereas these temperatures seem high, they are in general agreement with bore-hole temperatures and estimates from vitrinite-reflectance data.

The calcite cements have various textural relationships and are either earlier than, or contemporaneous with late, pore-filling anhydrite. Isotopic data indicate that the late anhydrite formed from a different process than the early, massive anhydrite. Given the approximate salinity of the brines from fluid-inclusion data, if the pore-filling anhydrite formed late in the burial history, the minimum temperature of anhydrite stability relative to gypsum would be between 75 and 120°C.

Acknowledgements

The authors are indebted to Alan Oldershaw, Bill Cutler and Roman Harrison of the Department of Geology and Geophysics, for their assistance and discussion. Asif Shakur of the Department of Physics, University of Calgary, did the isotopic analyses and was most co-operative. Discussions with Hans Machel, Eric Mountjoy and Jim Anderson aided in the interpretation and discussion of results. Comments by reviewers of the journal were useful. Hutcheon is grateful for financial support from N.S.E.R.C.

References

Bostick, N.H. (1979): Microscopic measurement of the level of catagenesis of solid organic matter in sedimentary rocks to aid exploration for petroleum and to determine former burial temperatures – a review. *In* Aspects of Diagenesis (P.A. Schoole & P.R. Schluger, eds.). *Soc. Econ. Paleontol. Mineral. Spec. Publ.* **26**, 17-43.

Chevron Standard Limited, Exploration Staff (1979): The geology, geophysics and significance of the Nisku Reef discoveries, West Pembina area, Alberta, Canada. *Can. Petroleum Geol. Bull.* **27**, 326-359.

Claypool, G.E., Holser, W.T., Kaplan, I.R., Sakai, H. & Zak, I. (1980): The age curves of sulfur and oxygen isotopes in marine sulfate and their mutual interpretation. *Chem. Geol.* **28**, 199-260.

Derro, G., Powell, T.G., Tissot, B. & McCrossan, R.G. (1977): The origin and migration of petroleum in the Western Canadian sedimentary basin, Alberta. *Geol. Soc. Can. Bull.* **262**.

Evamy, B.D. (1969): The precipitational environment and correlation of some calcite cements deduced from artificial staining. *J. Sed. Petrology* **39**, 787-793.

Keenan, J.H., Keyes, F.G., Hill, P.G. & Moore, J.G. (1969): *Steam Tables.* John Wiley and Sons, New York.

Oldershaw, A.E. & Scoffin, T.P. (1967): The source of ferroan and nonferroan calcite cements in the Halkin and Wenlock limestones. *Geol. J.* **5**, 309-320.

Potter, R.W., II & Clynne, M.A. (1978): Solubility of highly soluble salts in aqueous media. I. NaCl, KCl, $CaCl_2$, Na_2SO_4 and K_2SO_4 solubilities to 100°C. *J. Res. U. S. Geol. Surv.* **6**, 701-705.

Robie, R.A., Hemingway, B.S. & Fisher, J.R. (1978): Thermodynamic properties of minerals and related substances at 298.15K and 1 bar (10^5 pascals) pressure and at higher temperatures. *U. S. Geol. Surv. Bull* **1452**.

Robinson, R.A. & Stokes, R.H. (1959): *Electrolyte Solutions.* Butterworths, London.

Sasaki, A. & Krouse, H.R. (1969): Sulfur isotopes and the Pine Point lead-zinc mineralization. *Econ. Geol.* **64**, 718-730.

Wong, P.K. & Oldershaw, A. (1981): Burial cementation in the Devonian Kaybob Reef complex, Alberta, Canada. *J. Sed. Petrology* **51**, 507-520.

Received December 1981, revised manuscript accepted March 1982.